

## Equation of State of CO<sub>2</sub> Shock Compressed to 1 TPa

L. E. Crandall,<sup>1,2</sup> J. R. Rygg,<sup>1,2,3</sup> D. K. Spaulding,<sup>4</sup> T. R. Boehly,<sup>1</sup> S. Brygoo,<sup>5</sup> P. M. Celliers,<sup>6</sup> J. H. Eggert,<sup>6</sup> D. E. Fratanduono,<sup>6</sup> B. J. Henderson,<sup>1,2</sup> M. F. Huff,<sup>1,2</sup> R. Jeanloz,<sup>7</sup> A. Lazicki,<sup>6</sup> P. Loubeyre,<sup>5</sup> M. C. Marshall,<sup>1</sup> D. N. Polsin,<sup>1</sup> M. Zaghoo,<sup>1</sup> M. Millot,<sup>6</sup> and G. W. Collins<sup>1,2,3</sup>

<sup>1</sup>Laboratory for Laser Energetics, University of Rochester

<sup>2</sup>Department of Mechanical Engineering, University of Rochester

<sup>3</sup>Department of Physics and Astronomy, University of Rochester

<sup>4</sup>University of California, Davis

<sup>5</sup>Commissariat à l'énergie atomique et aux énergies alternatives

<sup>6</sup>Lawrence Livermore National Laboratory

<sup>7</sup>University of California, Berkeley

At terapascal pressures (10M atm), forces on atoms and molecules are comparable to their intrinsic quantum forces. Carbon dioxide is a simple molecular species with strong and stable chemical bonds at ambient conditions that exhibits complex phase transition behavior under increasing pressure and temperature. The physical, chemical, and thermodynamic behaviors of simple molecules comprising H, C, O, and N at hundreds of GPa and thousands of kelvin are vital to unraveling the dynamo, convective flow, and evolution of giant planets.<sup>1–3</sup> Additionally, CO<sub>2</sub> is an important by-product of reacted chemical explosives, and its polarity, conductivity, and diffusivity at high pressure dictate the reactive dynamics of these explosives.<sup>4,5</sup> The phase diagram of solid carbon dioxide has been extensively studied with heated diamond-anvil cells (DAC's) to 120 GPa (Refs. 6–11). This work demonstrates that the warm-dense-fluid regime of CO<sub>2</sub> is equally complex up to TPa pressures.

This work uses precompression and laser-driven shocks to explore the CO<sub>2</sub> equation of state (EOS) over a wide range of pressures and temperatures, extending to 1 TPa (10 Mbar) and 93,000 K (8 eV). CO<sub>2</sub> was precompressed to pressures up to 1.16 GPa in DAC's, attaining both liquid and solid initial states, and was then shock compressed. The temperature–pressure–density internal energy ( $T, P, \rho, E$ ) EOS and optical reflectance ( $R$ ) at 532 nm for these shocks were obtained with a velocity interferometer and an optical pyrometer. These data map a broad range of states from which thermodynamic derivatives were inferred, including the specific heat and the Grüneisen coefficient.

Combining these new data with previous results<sup>12–16</sup> and theoretical calculations<sup>17</sup> reveals a rich and complex phase diagram for CO<sub>2</sub>. The shocked fluid exhibits at least three linear slopes in the shock velocity versus particle velocity plane; this may indicate three distinct phases or two phases with a transition region. Optical reflectivity measurements reveal an insulator-to-conductor transition between 100 and 200 GPa with a carrier density of roughly 0.3 electrons/atom. The observed trend in specific heat suggests a complex bonded fluid with increasing molecular degrees of freedom up to 1 TPa as opposed to an atomic fluid. We find that state-of-the-art modeling needs refinement to match the observed reflectivity and compressibility behavior of CO<sub>2</sub>. High-pressure chemistry was once believed to be rather simple; this work reveals multiform behavior that is potentially quite general, as most of the known matter of the universe exists at high energy density ( $P > 100$  GPa).

These shocked CO<sub>2</sub> experiments were performed at the Omega Laser Facility.<sup>18</sup> CO<sub>2</sub> samples were precompressed to various initial pressures<sup>19</sup> using DAC's<sup>20,21</sup> to explore a family of Hugoniot. The velocity of the reflecting shock wave was measured throughout the shock transit of the entire experiment with a dual-channel velocity interferometer system for any reflector (VISAR).<sup>22</sup>

A quartz or fused-silica pusher was used as a reference<sup>23–28</sup> for impedance matching<sup>29</sup> at the pusher/CO<sub>2</sub> interface to determine the pressure and particle velocity of shocked CO<sub>2</sub>. Density and internal energy were then determined from the Rankine–Hugoniot conservation relations. Compressibility data is plotted in Fig. 1(b). As initial density increases, the CO<sub>2</sub> Hugoniot becomes stiffer. Density-functional-theory (DFT) calculations<sup>30</sup> agree well with the initially 1.17-g/cm<sup>3</sup> data [Fig. 1(b), blue circles, squares, and diamonds] (Refs. 12, 13, and 16), but the higher initial density CO<sub>2</sub> data [Fig. 1(b), green pentagons and triangles]<sup>14</sup> exhibit less compressibility than that model predicts between 50 and 500 GPa. More-recent LEOS (Livermore equation of state) fits [dashed lines in Fig. 1(b)]<sup>31</sup> match the OMEGA initial 1.4-g/cm<sup>3</sup> and 1.7-g/cm<sup>3</sup> data (green and red triangles), but they do not predict the increase in compressibility seen by Nellis *et al.* (blue squares)<sup>13</sup> above 30 GPa.

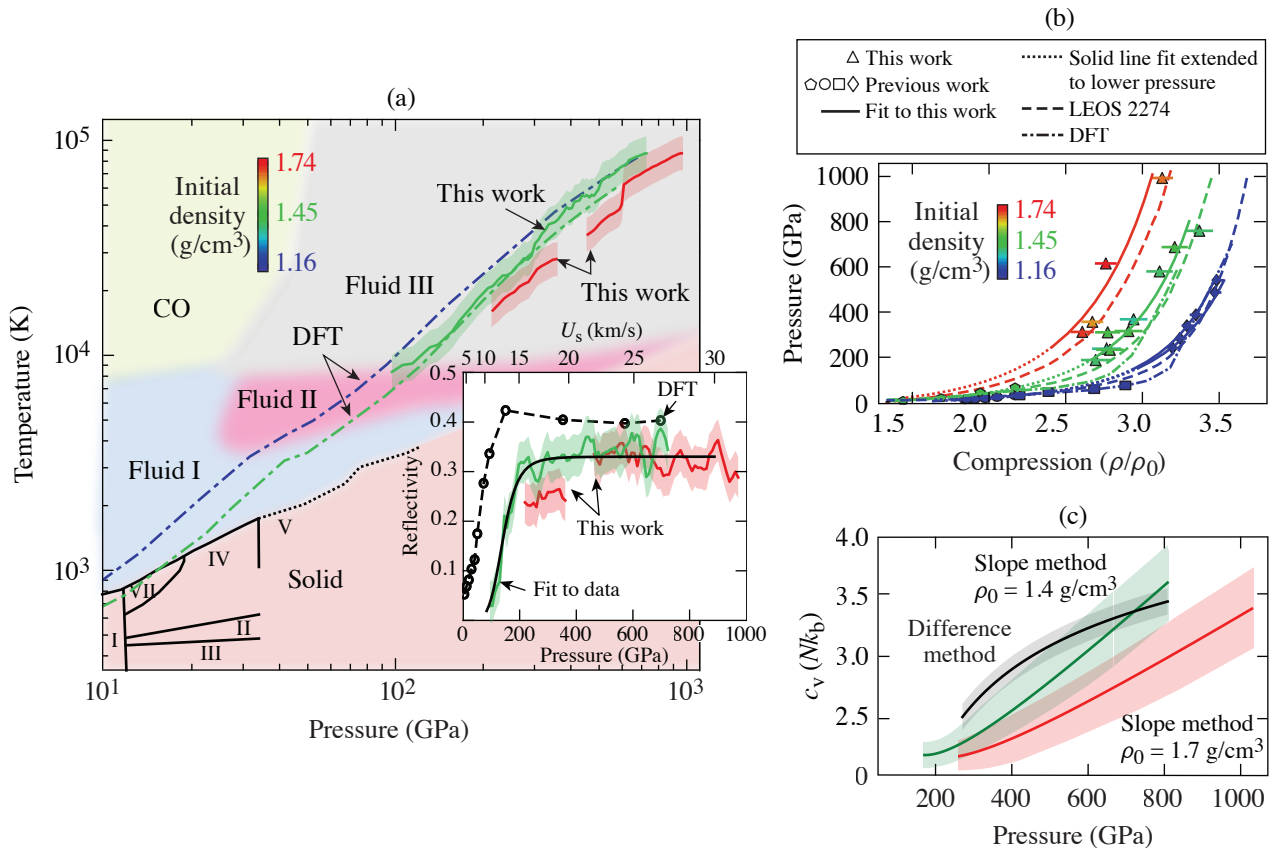


Figure 1

(a) Temperature versus pressure for shocked CO<sub>2</sub>. Color of all data refers to initial density as given by the color bar. Inset: Reflectivity versus pressure. Saturated reflectivity implies a constant carrier density above 200 GPa. (b) Pressure versus compression, representing disagreement between the compression data and state-of-the-art models. (c) Specific heat versus pressure. The increasing trend implies increasing degrees of freedom with increasing pressure and temperature. Together, reflectivity and specific heat trends imply a moderately ionized and complex bonded state at extreme pressure.

The self-emission (590 to 850 nm) from the shock was measured using streaked optical pyrometry (SOP).<sup>32</sup> The higher initial density Hugoniot is cooler than the lower initial density Hugoniot, and theoretical models<sup>30</sup> are consistent with our observed temperatures. The shock reflectivity at 532 nm [inset in Fig. 1(a)] is deduced from the VISAR amplitude and intensity as referenced to the known reflectivity of the quartz standard.<sup>25,33</sup> The reflectivity rises steeply from a few percent at 100 GPa to saturation at 32% above 200 GPa, lower than the theory-predicted saturation of 40%. The steep rise is a result of the insulator-to-conductor transition driven by increasing pressure and temperature. Previous theoretical work predicted the onset of metallization to occur as low as 20 GPa (Ref. 34). We propose that metallization begins in Fluid-III, above 100 GPa on the Hugoniot. A multiphase fluid regime is constructed in Fig. 1(a) based on trends in the shock velocity of CO<sub>2</sub> in conjunction with theoretical calculations<sup>17</sup> that predict a four-fluid system. The predicted boundaries of these fluids were adjusted to be consistent with the observed data.

Simultaneous temperature measurements allow one to calculate the isochoric specific heat [Fig. 1(c)]. The slope method<sup>33</sup> allows one to calculate the specific heat along the Hugoniot of initially liquid (1.4-g/cm<sup>3</sup>) and initially solid (1.7-g/cm<sup>3</sup>) CO<sub>2</sub>. The specific heat steadily increases from 200 GPa to 1 TPa for both initially liquid and solid CO<sub>2</sub>. The difference method, independent from the slope method, corroborates the trend of increasing specific heat. Increasing specific heat indicates increasing degrees of freedom (DOF's) in the fluid; because reflectivity is constant above 200 GPa, the increase in DOF's is not due to a rising carrier density. We conclude that the electrically conducting Fluid-III phase consists of a moderately ionized and bonded species of increasing chemical complexity, rather than a simple atomic fluid undergoing increasing ionization.

In summary, this work extends pressure and density measurements of the initially liquid and initially solid CO<sub>2</sub> Hugoniot to 1 TPa and provides the first temperature measurements of shocked CO<sub>2</sub> to 93,000 K. We propose a fluid phase diagram comprising at least three regimes to describe all existing shocked CO<sub>2</sub> data. Reflectivity and specific heat trends indicate that at pressures reaching 1 TPa, CO<sub>2</sub> is not likely a simple atomic fluid but instead a complex bonded and partially ionized species. Current models do not predict the observed compressibility and metallization behavior of high-pressure CO<sub>2</sub>. This work demonstrates the rich behavior of nominally simple materials at high energy density and invites further inquiry into the chemistry of warm dense matter.

This material is based upon work supported by the Department of Energy National Nuclear Security Administration under Award Number DE-NA0003856, the University of Rochester, and the New York State Energy Research and Development Authority. A portion of this work was conducted at Lawrence Livermore National Laboratory under Contract Number DE-AC52-07NA27344.

1. T. Guillot, *Science* **286**, 72 (1999).
2. C. Cavazzoni *et al.*, *Science* **283**, 44 (1999).
3. S. Stanley and J. Bloxham, *Nature* **428**, 151 (2004).
4. M. van Thiel and F. H. Ree, *J. Appl. Phys.* **62**, 1761 (1987).
5. V. V. Chaban, E. E. Fileti, and O. V. Prezhdo, *J. Phys. Chem. Lett.* **6**, 913 (2015).
6. K. F. Dziubek *et al.*, *Nat. Commun.* **9**, 3148 (2018).
7. F. Datchi and G. Weck, *Z. Kristallogr.* **229**, 135 (2014).
8. C.-S. Yoo, *Phys. Chem. Chem. Phys.* **15**, 7949 (2013).
9. K. D. Litasov, A. F. Goncharov, and R. J. Hemley, *Earth Planet. Sci. Lett.* **309**, 318 (2011).
10. V. M. Giordano *et al.*, *J. Chem. Phys.* **133**, 144501 (2010).
11. V. M. Giordano, F. Datchi, and A. Dewaele, *J. Chem. Phys.* **125**, 054504 (2006).
12. G. L. Schott, *High Press. Res.* **6**, 187 (1991).
13. W. J. Nellis *et al.*, *J. Chem. Phys.* **95**, 5268 (1991).
14. V. N. Zubarev and G. S. Telegin, *Sov. Phys.-Dokl.* **7**, 34 (1962).
15. Zubarev and Telegin<sup>14</sup> report two different initial densities for their solid CO<sub>2</sub>: 1.45 and 1.54 g/cm<sup>3</sup>. Cited in Schott<sup>12</sup> are “verbal inquires and replies conveyed through C. L. Mader and A. N. Dremin, ca. 1983” that confirm that 1.54 g/cm<sup>3</sup> is a misprint, and the initial density of the data published by Zubarev and Telegin is 1.45 g/cm<sup>3</sup>.
16. S. Root *et al.*, *Phys. Rev. B* **87**, 224102 (2013).
17. B. Boates, A. M. Toweldeberhan, and S. A. Bonev, *Proc. Natl. Acad. Sci.* **109**, 14808 (2012).

18. T. R. Boehly *et al.*, *Opt. Commun.* **133**, 495 (1997).
19. G. J. Piermarini *et al.*, *J. Appl. Phys.* **46**, 2774 (1975).
20. J. Eggert *et al.*, *Phys. Rev. Lett.* **100**, 124503 (2008).
21. P. M. Celliers *et al.*, *Phys. Rev. Lett.* **104**, 184503 (2010).
22. P. M. Celliers *et al.*, *Rev. Sci. Instrum.* **75**, 4916 (2004).
23. M. D. Knudson and M. P. Desjarlais, *Phys. Rev. B* **88**, 184107 (2013).
24. M. P. Desjarlais, M. D. Knudson, and K. R. Cochrane, *J. Appl. Phys.* **122**, 035903 (2017).
25. S. Brygoo *et al.*, *J. Appl. Phys.* **118**, 195901 (2015).
26. C. A. McCoy *et al.*, *J. Appl. Phys.* **119**, 215901 (2016).
27. C. Meade and R. Jeanloz, *Phys. Rev. B* **35**, 236 (1987).
28. R. G. Kraus *et al.*, *J. Geophys. Res. Planets* **117**, E09009 (2012).
29. Ya. B. Zel'dovich and Yu. P. Raizer, in *Physics of Shock Waves and High-Temperature Hydrodynamic Phenomena*, edited by W. D. Hayes and R. F. Probstein (Dover Publications, Mineola, NY, 2002).
30. B. Boates *et al.*, *J. Chem. Phys.* **134**, 064504 (2011).
31. C. J. Wu *et al.*, *J. Chem. Phys.* **151**, 224505 (2019).
32. J. E. Miller *et al.*, *Rev. Sci. Instrum.* **78**, 034903 (2007).
33. D. G. Hicks *et al.*, *Phys. Rev. Lett.* **97**, 025502 (2006).
34. C. Wang and P. Zhang, *J. Chem. Phys.* **133**, 134503 (2010).